Astron. Astrophys. 302, 658–664 (1995)

ASTRONOMY AND ASTROPHYSICS

Distribution of ionized gas in X-ray bright early-type galaxies*

K.P. Singh[1], P.N. Bhat[1], T.P. Prabhu[2], and A.K. Kembhavi[3]

[1] Tata Institute of Fundamental Research, Bombay 400 005, India
[2] Indian Institute of Astrophysics, Bangalore 560 034, India
[3] Inter-University Centre for Astronomy and Astrophysics, Pune 411 007, India

Received 7 February 1994 / Accepted 2 February 1995

Abstract. We report imaging observations of Hα+[N II] nebulosities in seven early type galaxies viz., NGC 1399, NGC 1600, NGC 2563, NGC 4203, NGC 4636, NGC 4753 and NGC 5044. These are primarily X-ray bright galaxies which are the dominant members of nearby groups. Many of these galaxies have X-ray cooling flows. The results are based on CCD surface photometry carried out using a broad-band filter R, and a narrow band filter appropriate for the red-shifted Hα+[N II] emission. We present the integrated Hα luminosities in these galaxies and examine various emission mechanisms. The observed Hα luminosity implies a mass of $\sim 10^5\,M_\odot$ in the ionized gas. We suggest that photo-ionization by young stars is a viable emission mechanism and star formation due to accretion events or mergers may be common in these galaxies.

Key words: galaxies: elliptical and lenticular; cooling flows; ISM; interactions

1. Introduction

Optical spectroscopic observations have revealed that nearly 40% of elliptical galaxies show faint emission lines indicating the presence of warm (10^4 K) ionized gas (Phillips et al. 1986). These emission line spectra have the characteristics of LINERS (Low Ionization Nuclear Emission Regions) wherein the lines from singly ionized species are strong relative to H II regions and higher ionization lines are weak relative to those in the active galactic nuclei. This has led to the suggestion that such spectra are typically produced by low velocity ($< 100\,\mathrm{km\,s^{-1}}$) shocks or photo-ionization by a dilute power-law continuum (Heckman 1987).

There have been attempts in recent years to map the emission line region and/or estimate the total emission-line flux through imaging observations. We list a few of the often quoted surveys. Demoulin-Ulrich et al. (1984) reported observations of spatial distributions, the velocity field and the line intensities in a sample of 12 nearby normal elliptical galaxies. Ionized gas regions extending 1–3 kpc in extent were found in 6 of them. Later Kim (1989) observed 26 infrared-bright ellipticals and mapped the Hα emission in 15 galaxies. More recently, Trinchieri & di Serego Alighieri (1991), hereafter TdSA, detected emission regions in ten early-type galaxies out of the 13 galaxies with known X-ray fluxes. A similar study of 46 galaxies by Shields (1991) led to the detection in 18 objects. Buson et al. (1993) observed 15 early-type galaxies with known extended emission-line regions. Goudfrooij et al. (1994) imaged a large number of Shapley-Ames galaxies and detected Hα emission in more than half of them. The total Hα luminosities estimated by these studies range between 10^{38}–10^{41} erg s^{-1} with implied mass of ionized hydrogen in the range 10^3–$10^6\,M_\odot$. The origin of the gas, its ultimate fate, and excitation mechanisms are not fully understood, however (Macchetto & Sparks 1992).

It is now well established that groups and clusters of galaxies are luminous X-ray sources, and that the X-ray emission, centered on bright early type galaxies, is extended and dominated by emission from hot gas (Fabbiano et al. 1992; Kim et al. 1992). In about 30% of the clusters studied, cooling time for the gas in the core of the cluster is less than the Hubble time H_0^{-1} and this leads to a cooling flow on to the central galaxy (Fabian et al. 1991; Fabian 1994). Optical line emission is usually found to be present in the cooling flow galaxies and shows a dependence on the X-ray luminosity (TdSA). It has also been shown that a large fraction of the bright early type galaxies have high Hα+[N II] emission line luminosities which correlate with stellar luminosities (La Valley et al. 1992). The investigations of line emissions in the dominant members of X-ray bright clusters can, therefore, be extremely interesting as it covers many topics e.g., inter-relationship of different gas phases, cooling flows, frequency and relevance of mergers in galaxy evolution, stellar evolution, star formation etc. With these aims in view, we are imaging the faint emission nebulosities and studying the properties of the warm gas viz., mass, luminosity, extent and structure.

We have carried out CCD observations of early-type (mostly elliptical) galaxies which are in small nearby groups. In this pa-

Send offprint requests to: P.N. Bhat

* Based on observations using Vainu Bappu Telescope, VBO, Kavalur

Table 1. The sample

Galaxy name	Morphological type (RC3)[f]	Blue magnitude (RC3)[f]	Distance[a] (Mpc)	Other information[b,c,d,e]
NGC 1399	E1	10.55	27.2	Fornax Cluster, HG17, CF
NGC 1600	E3	11.93	90.3	NGC1600 group, CF
NGC 2563	SO	13.24	96.1	Cancer cluster, CF
NGC 3607	SO	10.82	32.0	N3607 Group, HG56, Dust rings
NGC 4203	SAB0	11.80	15.6	GH94
NGC 4636	E0	10.43	27.3	HG41, CF
NGC 4753	I0	10.85	24.3	HG41, Extensive Dust lanes
NGC 5044	E0	11.72	62.5	HG39, CF

[a] Distances are from Fabbiano et al. (1992).
[b] HG : Group of galaxies from the Catalog by Huchra & Geller (1982).
[c] GH : Group of galaxies from the Catalog by Geller & Huchra (1983). Also see Vennik (1986) for the N3607 group.
[d] CF : Cooling flow galaxy (Thomas et al. 1986; David et al. 1993).
[e] See Singh et al. 1994 for dust rings in NGC 3607.
[f] RC3: Third Reference Catalogue of Bright Galaxies.

per, we report our observations of seven such galaxies viz., NGC 1399, NGC 1600, NGC 2563, NGC 4203, NGC 4636, NGC 4753 and NGC 5044. Results from our observations of NGC 3607 have already been reported (Singh et al. 1994), however, we have included them here for the sake of completeness. Information about their exact types, magnitude, distance and group membership is listed in Table 1. These galaxies were selected by virtue of their X-ray emission (Fabbiano et al. 1992). These are also the dominant or central members of their respective groups. X-ray emission from five of the galaxies in our sample has been analyzed for cooling flows and inflow rates ranging from 0.4 to $20.0\,M_{\odot}\,yr^{-1}$ have been detected (Stanger & Warwick 1986; Thomas et al. 1986; David et al. 1993).

We have obtained color maps, and found evidence for circum-nuclear shells and dust lanes in almost all the galaxies in our sample, suggesting the possibilities of galaxy-galaxy interactions or mergers. Some of these results will be presented elsewhere. We present here the maps of Hα nebulosities in these galaxies based on observations with narrow-band filters and a broad-band R filter. We estimate the mass of the ionized gas, and explore the emission mechanisms and sources of energy supply for the gas.

2. Observations

The galaxies were imaged using a GEC P8603/A front-illuminated CCD at the prime focus of the 2.3 m Vainu Bappu Telescope (VBT) at Kavalur. The images were obtained through a broad-band R filter and narrow-band filters selected appropriately for the target galaxy based on its redshift so as to cover the Hα emission. The details of the observations are given in Table 2. The sky conditions for the data reported here were by and large photometric. The standard stars in the "dipper asterism" region of the open cluster M67 and standard stars from Landolt (1983) and Kilkenny & Menzies (1989) were observed for calibrating the CCD. Spectrophotometric standard stars (Stone 1977) in the neighboring regions of the sky were observed for calibrating the narrow-band filter data. The Full Width Half Maximum (FWHM) of the point spread function (psf) was $\simeq$ 2–2.4 arcsec in both the filters. The details of the CCD camera and its standardization using the M67 star cluster have been reported by Bhat et al. (1990, 1992) and Anupama et al. (1994). In brief, the image scale on the CCD is 0.6 arcsec pixel^{-1} at the $f/3.25$ prime focus of the VBT and the field of view is 5.7×3.8 arcmin^2. The read-out noise of the CCD is $\sim$ 10 electrons and the gain setting corresponds to $\sim$ 4 electrons per CCD count (ADU) (Prabhu et al. 1992).

3. Analysis and results

We analyzed the CCD images using standard tasks in the IRAF [1] software package. The image frames and flat-field frames were bias subtracted using the bias frames obtained very close to the observations. The best flat fields obtained from the twilight and the dawn sky were used for flat-field corrections. To improve the signal-to-noise ratio and to reduce the pattern noise seen at very low levels in the images due to electronic interference noise, we employed an approximation of the Weiner filter using the fast Fourier transforms as explained in detail by Wampler (1992). The subsequent analysis utilized the final corrected images.

Both galaxies and standard stars were observed close to zenith. Since for program galaxies the atmospheric extinction in the adopted pass bands should not exceed 0.05 mag, no extinction correction has been made.

3.1. Hα+[N II] emission

The surface brightness maps of the galaxies in the Hα + [N II] line emission were obtained by subtracting the continuum im-

[1] IRAF is distributed by the National Optical Astronomy Observatories, which is operated by the Association of Universities, Inc. (AURA) under cooperative agreement with the National Science Foundation

Table 2. Details of Observations

NGC No.	Heliocenteric radial velocity ($km\,s^{-1}$)	Observation date	Seeing (arcsec)	Filters name/ Central λ (Å)	Width ($\Delta\lambda$) narrow-band (Å)	Exposure time (s)
1399	1447	1993 January 19	2.4	R		720
			2.5	6584	100	1800
1600	4718	1993 January 18	1.9	R		900
			2.0	6680	102	1800+1800
2563	4674	1993 January 18	1.9	R		900
			2.0	6680	102	1800+1800
3607	935	1993 January 19	2.0	R		480
			2.0	6584	100	1800
4203	1044	1993 April 16		R		600+600
				6564	99	1800
4636	927	1993 April 17	2.4	R		600
			2.5	6564	99	1800+1200
4753	1237	1993 April 17	2.4	R		720
			2.5	6564	99	1800
5044	2692	1993 January 20	2.7	R		600
			3.0	6680	102	1800

Table 3. Parameters of the ionized gas

Galaxy name NGC	Log $L_{H\alpha+[NII]}$ ($erg\,s^{-1}$)	log $L^{a}_{H\alpha}$ ($erg\,s^{-1}$)	log L^{b}_{x} ($erg\,s^{-1}$)	Gas extent diameter (kpc)	Electron density[c] (cm^{-3})	M_{gas} ($10^5\,M_\odot$)
1399	40.98	40.53	42.31	4.75	375	2.08
1600	40.36	39.91	41.95	3.9	224	0.83
2563	<40.30	<39.90	42.12	–	–	–
3607	40.63	40.18	40.88	2.8	425	0.82
4203	40.82	40.37	40.96	2.0	740	0.73
4636	40.20	39.75	41.65	2.4	306	0.42
4753	40.55	40.10	40.08	2.5	434	0.67
5044	41.66	41.21	43.17	6.4	609	6.13

[a] Derived values : see the text for assumptions.
[b] Fabbiano et al. (1992).
[c] Assuming filling factor of $5\,10^{-6}$ and scale height of 250 pc for the gas disk.

age in the R filter, after proper scaling and realignment, from the image taken with the narrow-band filter. The scaling factor was estimated from the relative efficiencies of the narrow-band filter and R filter, derived from the observations of the spectrophotometric and photometric standards, and assuming that the stellar component in the galaxy has a similar spectrum. Such an approximation can affect, to some extent, the derived emission line fluxes and the observed morphology of the line-emitting region. The resultant images of the line emission smoothed using a median filter with a 3×3 kernel, are shown in Fig. 1 as contour plots. The peak of the continuum emission is marked with 'plus' sign in the figures. The Hα+[N II] emission is mostly concentrated around the nuclear region but is clearly resolved. In general, it is extended with an elliptical distribution with somewhat higher eccentricity compared to the isophotes in continuum images. The position angle determination of the extended line emission has large errors. In general, we find that the differences in the position angle of the line image versus the continuum image are small and not very significant, in our sample. The Hα+[N II] fluxes were measured using a circular aperture centered on the nucleus and big enough to encompass all the line emission. The size of the aperture used is, therefore, different for different galaxies. We employed DAOPHOT (Stetson 1987) package for the purpose. The total Hα+[N II] luminosities derived from the fluxes and using the distances given by Fabbiano et al. (1992) are given in Table 3. Assuming a mean value of 1.38 for [N II]λ6583/Hα (Phillips et al. 1986), and the ratio of 3 for $\lambda6583/\lambda6548$ we obtain a corrected Hα luminosities which are given in Table 3. The extent of the ionized gas in each galaxy is also listed in Table 3.

Hα luminosities are not corrected for the foreground Galactic extinction which appears to be negligible (Burstein & Heiles

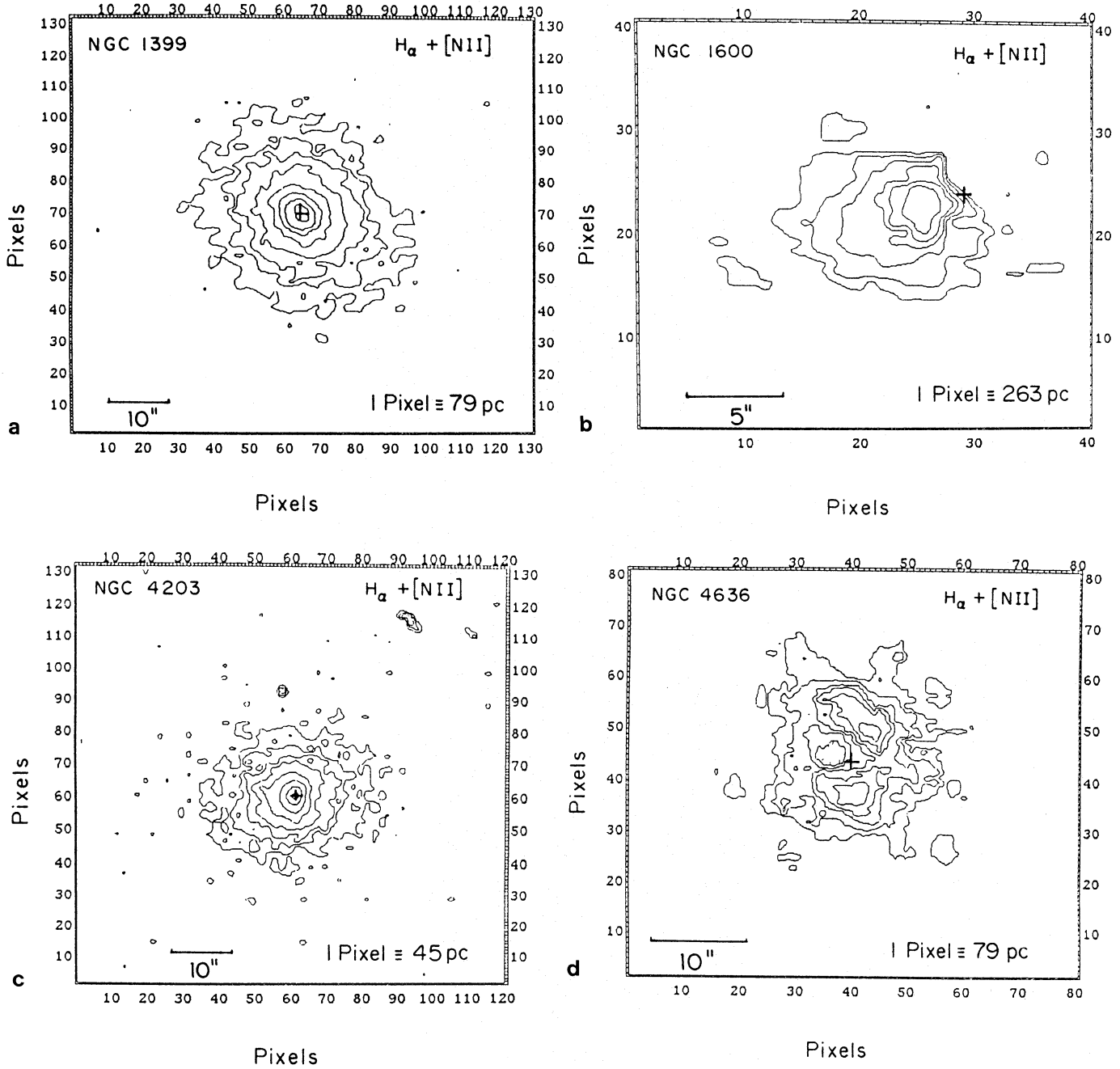

Fig. 1a–f. Surface Brightness maps of Hα + [N II] emission. The contour levels are **a** 3.4, 6.1, 8.7, 14.0, 24.7, 37.9, 51.2 and 64.5 $\times$ 10^{-16} erg cm^{-2} s^{-1} arcsec^{-2} for NGC 1399; **b** 0.9, 1.44, 2.16, 2.9, 3.6 and 4.5 $\times$ 10^{-16} erg cm^{-2} arcsec^{-2} for NGC 1600; **c** 1.3, 2.2, 3.2, 4.8, 8.0, 16.0, 32.0 and 48.2 $\times$ 10^{-15} erg cm^{-2} s^{-1} arcsec^{-2} for NGC 4203; **d** 4.5, 6.8, 9.1, 11.3, 14.2 and 17.0 $\times$ 10^{-16} erg cm^{-2} s^{-1} arcsec^{-2} for NGC 4636; **e** 6.6, 9.4, 14.2, 18.9, 28.4, 47.3, 74.8 and 103.9 $\times$ 10^{-16} erg cm^{-2} s^{-1} arcsec^{-2} for NGC 4753; **f** 1.0, 1.6, 2.1, 2.8, 4.3, 5.7, 8.7 and 11.7 $\times$ 10^{-15} erg cm^{-2} s^{-1} arcsec^{-2} for NGC 5044. The peak of the continuum emission is marked with 'plus' sign in the figures. East is towards the top and North is towards the right approximately. (1 pixel = 0.6 arcsec)

1984). No attempt was made to remove the effect of internal absorption.

The FIR luminosities of the galaxies in our sample indicate the presence of significant amount of dust so as to make the extinction correction to Hα luminosities significant (Roberts et al. 1991). Future observations in the Hβ band would be necessary to make these corrections.

3.2. Comments on individual galaxies

NGC 1399: The line emission is peaked on the nucleus and extended to a radius of $\simeq$ 18 arcsec corresponding to $r \simeq 2.4$ kpc. The shape of the nebulosity is symmetrical with respect to the continuum light.

NGC 1600: The line emission peak is offset towards the south-

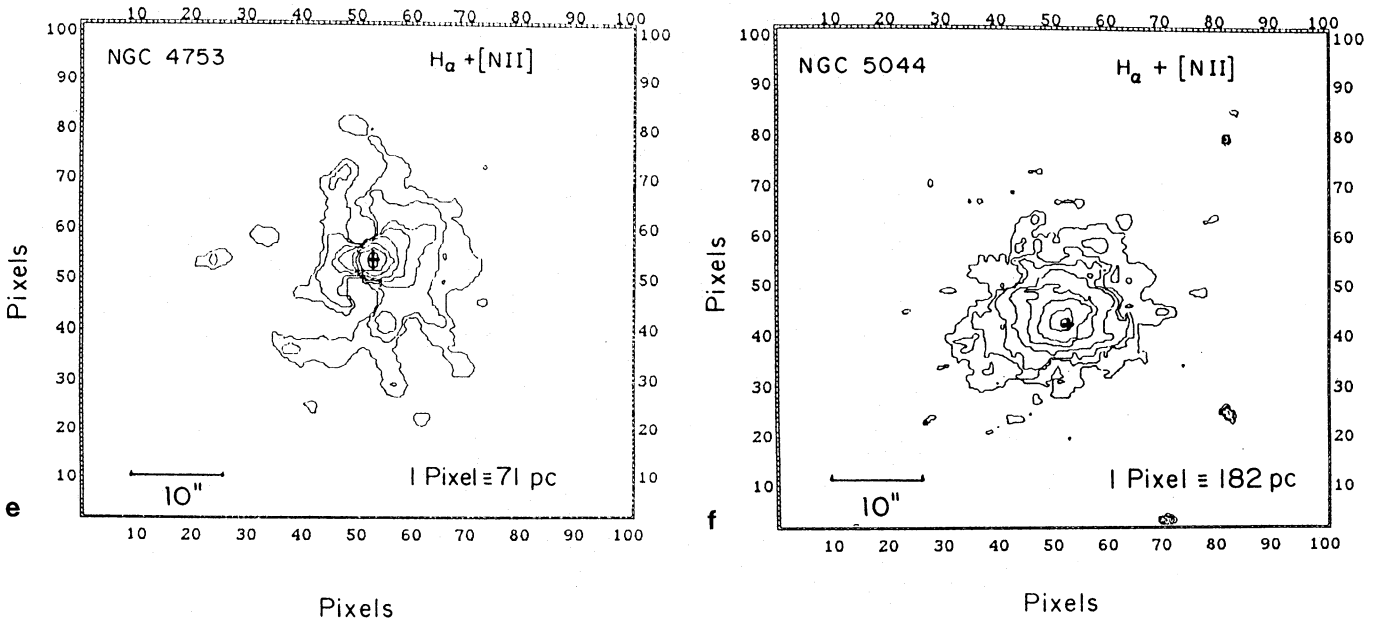

Fig. 1e and f.

west from the center of the continuum image, and extended asymmetrically in the south-westerly direction with a radius of $\simeq$ 5 arcsec corresponding to $\simeq$ 2 kpc.

NGC 2563: No line emission was detected from this galaxy.

NGC 4203: The line emission is concentrated on the nucleus and extended symmetrically to a radius of $\simeq$ 13.5 arcsec corresponding to $r \simeq 1.0$ kpc.

NGC 4636: Emission line nebulosity shows an unusual ring-like structure with a minimum or a 'hole' very close to the middle but slightly offset from the continuum peak. The line emission extends to a radius of $\simeq$ 9 arcsec corresponding to r $\simeq$ 1.2 kpc.

NGC 4753: The line emission is peaked on the nucleus and extended filamentary structure is seen. The maximum size in the east-west direction has a radius of $\simeq$ 10.5 arcsec corresponding to $\simeq$ 1.25 kpc. The lack of line emission coincides with the dust lanes.

NGC 5044: The line emission is concentrated on the nucleus and extended somewhat asymmetrically to a radius of $\simeq$ 10.5 arcsec corresponding to r $\simeq$ 3.2 kpc.

3.3. Comparison with previous measurements

Imaging the distribution of line emission is of fairly recent origin and a direct comparison of emission-line luminosity measurements with those published in the literature is somewhat complicated by the different aperture sizes and distances used. All the galaxies observed by us have previous detections or upper limits of Hα + [N II] luminosities. After bringing them to the scale of distances used by us, we find that our detection of NGC 1600 is close to the upper limit quoted by Shields (1991), and our luminosity is 30% higher than estimated by TdSA. Our upper limit for NGC 2563 is slightly lower than Shields'. There is an excellent agreement between our estimate and that of Shields in the case of NGC 3607. In the case of NGC 4636, our estimate is about 60% higher than Shields', whereas a factor of two less than that of Buson et al. (1993). Our estimate is 80% higher than that of Goudfrouij et al. (1994) in the case of NGC 5044, and a factor of 2.7 higher than that of Shields in the case of NGC 4753. The two cases of serious discrepancy are those of NGC 1399 for which Goudfrooij et al. obtain an order of magnitude lower flux and NGC 4203 where Shields obtains an order of magnitude lower flux. Since we had observed NGC 1399 and NGC 3607 on the same night, considering the good agreement in the case of the latter, we are confident about having detected a significant amount of ionized gas in the giant elliptical in the Fornax Cluster. The differences in the estimates of different authors exemplify the difficulty in an accurate subtraction of continuum from line images. We believe that our estimates are accurate to a factor of two.

Our map of NGC 1600 is in good agreement with TdSa in shape and size. The size, shape and unusual ring-like morphology of the gas in NGC 4636 is consistent with the map published by Demoulin-Ulrich et al. (1984) and Buson et al. 1993. The distribution of ionized gas in NGC 4203 is presented here for the first time. Our map of NGC 4753 reaches a larger radius compared to the map of Shields (1991). Similarly, our maps extend further in the case of NGC 1399 and 5044 in comparison with the maps of Goudfrooij et al. (1994).

4. Discussion

4.1. Extent and mass of the ionized gas

All galaxies in our sample, except NGC 2563, are detected to have significant line emission. The sizes and luminosities of the ionized gas are given in Table 3. The sizes are in the range

2.0–2.5 kpc in NGC 3607, 4203, 4636 & 4753, and 4–6 kpc in NGC 1399, 1600 and 5044. Assuming that the gas is distributed in a disk-like geometry with a scale height of 250 pc, and that the filling factor is $5\,10^{-6}$ then for the Case B recombination (Osterbrock 1989) we can estimate the electron density and mass of the gas. The values of the electron density and mass, thus derived (see Table 3) range from 200–700 cm^{-3} and 4–60 10^4 $M_\odot$, respectively.

We expect the gas to be rotationally supported, and the surface density to be decreasing exponentially with radius as in the case of gaseous disks in galaxies. There is some evidence of an exponential disk in the case of N1399, 4203, 5044 which show symmetric distribution of gas, the scale lengths being 2.8, 2.1 and 13.6 kpc, respectively. These scale lengths are comparable to the effective radii of stellar distribution. N3607 also shows an exponential disc, but with a scale-length of only 400 pc which is about sixth of the effective radius. The ionized gas in N3607 would hence appear to be a nuclear component.

4.2. Emission mechanisms

Several mechanisms have been studied by earlier investigators in order to explain the extended Hα emission in early type galaxies (cf. Singh et al. 1994). Ionization due to recombination in cooling flow fails to account for the observed emission nebulosities unless the recombination rate is increased by 10^2 to 10^3 times. Heat conduction, though adequate in some galaxies with small ratio of L_{H_α} to L_x as in NGC 4696 (Sparks et al. 1989), is found to be insufficient to match the cooling efficiency of the 10^4 K gas in NGC 3607 (Singh et al. 1994), NGC 4203 and 4753. Photoionization thus offers the only possible mechanism to account for the emission.

Photoionization by post-asymptotic giant branch (PAGB) stars (TdSA) is a viable mechanism which can marginally account for the Hα emission (Singh et al. 1994). Buson et al. (1993) find that the radio-continuum power is 10–15 times the average in their sample of early-type galaxies with detectable Hα emission and suggest that an active nucleus plays a part in ionizing the gas. The total Hα luminosities measured by us as well as by Buson et al. are on an average an order of magnitude lower than the nuclear emission from low-luminosity AGN (cf. Shuder 1981). Thus if the nuclear activity is mainly responsible for the ionization and the parameters affecting the emission-line spectrum produce a constant equivalent width, the non-thermal continuum flux of the nucleus should be similarly fainter. In this respect, it will be of interest to obtain information on the nuclei through spectrophotometry, though Heckman et al. (1989) have argued that the processes associated with nuclear activity are generally inadequate to explain the emission.

We examine in some detail the possibility of photoionization by young stars. The minimum number of Lyman-continuum photons Q (photons s^{-1}) required to produce the observed Hα luminosity is $7.32\,10^{11}\,L_{H\alpha}$ (erg s^{-1}) (Case B, Osterbrock 1989). This implies $Q = (4.1\text{–}118.7)\,10^{51}$ photons s^{-1}. A population of hot young stars can supply these photons. Evidences for such stars in many ellipticals is provided through spectroscopy of underlying population by Johnstone et al. (1987). These stars could derive from a small fraction of the mass presumably deposited by cooling flows in the form of very low mass stars. Ionizing radiation for an IMF with a slope of 2.5, a lower cutoff at 1 $M_\odot$, and an upper cutoff at 30 $M_\odot$ is $6\,10^{45}$ photons s^{-1} $M_\odot{}^{-1}$ (Mayya 1993, 1995). The total mass in the young stars needed to explain the observed Hα emission is then found to be (0.7–20) 10^6 $M_\odot$. The e-folding time for ionizing radiation due to evolution of the burst is $5.5\,10^6$ yr. Hence, either we are looking at a young burst at the present epoch, or witnessing continuous star-formation at a rate of 0.1–3.6 $M_\odot$ yr^{-1}. Increasing the upper mass limit reduces the implied star-formation rate. Under similar assumptions, SFR can be estimated also from FIR luminosities (Brosch & Loinger 1991). The observed range of FIR luminosities correspond to $2\,10^8$–$5\,10^9\,L_\odot$ (Lonsdale et al. 1989; Roberts et al. 1991) and imply a star-formation rate of 0.1–3 $M_\odot$ yr^{-1}, a figure suggestively similar to the earlier estimate. We thus conclude that ongoing star-formation with upper cutoff of about 30 $M_\odot$ is a viable mechanism to explain the observed Hα emission.

4.3. Gas supply

The cooling time of the warm gas is very short and besides the dust also cannot survive for too long in these environments. Therefore, both dust and neutral gas need to be replenished frequently. In the case of NGC 3607, there is a good evidence, from rotation curve, of interaction with the gas rich neighbor NGC 3608 (Jedrzejewski & Schechter 1988) which could also be the supplier of gas and dust. Shells and ripples in a number of ellipticals have also been observed (Malin & Carter 1983). Theories involving collision and subsequent merger of a galaxy with a bigger galaxy can, however, explain many of the features in these shells. This suggests significant ongoing merger activity and star formation in these galaxies (Hernquist & Quinn 1988, 1989).

5. Conclusions

The 7 out of 8 galaxies in our sample exhibit significant ionized gas extending from 2 to 6 kpc from the nucleus. A majority of them show a significant concentration at the nucleus while in NGC 1600 the peak is offset with respect to that in continuum image. In some cases the distribution extends symmetrically around the nucleus while in two cases it extends asymmetrically.

An amount of $4\,10^4$ to $6\,10^5$ $M_\odot$ of ionized gas has been detected by us in the central regions of galaxies. The implied SFR is 0.1 to 3.6 $M_\odot$ yr^{-1}, over the last 5.5 Myr for a Salpeter IMF between 1 and 30 $M_\odot$. This figure is in excellent agreement with FIR emission vindicating our suggestion that star formation is a viable mechanism for ionization of gas and heating dust. One would, however, conclude that $7\,10^5$ to $2\,10^7$ $M_\odot$ of gas is converted to stars during the past 5.5 Myr. This mass is comparable to the amount of gas estimated as 100 times the mass of dust at 30K (M_{dust} = $5\,10^4$–$1\,10^6$ $M_\odot$). Thus, unless a top-heavy star formation is assumed, leading to a decrease in

SFR estimates both from Hα and FIR luminosities, implied star formation efficiency would be very high.

Acknowledgements. We thank the Director of the Indian Institute of Astrophysics and the Time Allotment Committee for allotting the dark nights for our observations. We are grateful to the staff of Indian Institute of Astrophysics, Bangalore for the maintenance of the CCD system. We thank G. Selvakumar and M. Ganesan for their assistance during the observations. This research has made use of the NASA/IPAC Extragalactic Database (NED) which is operated by the Jet Propulsion Laboratory, Caltech, under contract with the National Aeronautics and Space Administration.

References

Anupama G.C., Kembhavi A.K., Prabhu T.P., Singh K.P., Bhat P.N. 1994, A&AS 103, 315
Bertola F., Buson L.M., Zeilinger W.W., 1992, ApJ 401, L79
Bhat P.N., Kembhavi A.K., Patnaik K., Patnaik A.R., Prabhu T.P., 1990, Indian J. Pure Appl. Phys. 28, 649
Bhat P.N., Singh K.P., Prabhu T.P., Kembhavi A.K., 1992, J. Astron. Astrophys. 13, 293
Bregman J.N., Hogg D.E., Roberts M.S., 1992, ApJ 387, 484
Brosch N., Loinger F., 1991, A&A 249, 327
Burstein D., Heiles C., 1984, ApJS 54, 33
Buson L.M., Sadler E.M., Zeillinger W.W., et al., 1993, A&A 280, 409
David L.P., Jones C., Forman W., Daines S., 1994, ApJ 428, 544
de Vaucouleurs G., de Vaucouleurs A., Corwin Jr. H.G., et al., Third reference Catalogue of Bright Galaxies, Springer Berlin Heidelberg New York (RC3)
Demoulin-Ulrich M.-H., Butcher H.R., Bokesenberg A., 1984, ApJ 285, 527
Fabian A.C., Nulsen P.E., Canizares C.R., 1991, A&AR 2, 191
Fabian A.C., 1994, ARA&A 32, 277
Fabbiano G., Kim D.-W., Trinchieri G., 1992, ApJS 80, 531
Geller M.J., Huchra J.P., 1983, ApJS 52, 61
Goudfrooij P., Hansen L., Jorgensen H.E., Norgaard-Nielsen H.U., 1994, A&AS 105, 341
Heckman T.M., 1987, IAU Symposium 121, Observational Evidence of Activity in Galaxies, Khachikian E., Fricke K., Melnick J. (eds.), Reidel, Dordrecht, p. 421
Heckman T.M., Baum S.A., van Breugal W.J.M., McCarthy P., 1989, ApJ 338, 48
Hernquist L., Quinn P.J., 1988, ApJ 331, 682
Hernquist L., Quinn P.J., 1989, ApJ 342 1
Huchra J., Geller M., 1982, ApJ 257, 423
Jedrzejewski R., Schechter P.L., 1988, ApJ 330, L87
Johnstone R.M., Fabian A.C., Nulsen P.E., 1987, MNRAS 224, 75
Kilkenny D., Menzies J.W., 1989, S. African Astron. Obs. Circ. No. 13, 25
Kim D.-W., 1989, ApJ 346, 653
Kim D.-W., Fabbiano G., Trinchieri G., 1992, ApJS 80, 645
Lada C.J., 1987, in: IAU Symp. 115: Star-forming Regions, Peimbert M., Jugaku J. (eds.), Reidel, Dordrecht, p. 1
Landolt A.U., 1983, AJ 88, 439
LaValley M., Isobe T., Feigelson E.D., 1992, Proc. First Ann. Conf. on Astron. Data Analysis Software and Systems, ASP, San Francisco, Worrall et al. (eds.)
Lonsdale C.J., Helou G., Good J.C., Rice W., 1989, Cataloged Galaxies and Quasars Observed in the IRAS Survey, JPL D-1932
Macchetto F., Sparks W.B., 1992, The Warm Component of the ISM of Elliptical Galaxies. In: Longo G., Capaccioli M., Busarello G. (eds.), Morphological and Physical Classification of Galaxies. Kluwer, Dordrecht, p. 191
Malin D.F., Carter D., 1983, ApJ 274, 534
Mayya Y.D., 1993, Ph. D. Thesis, Indian Institute of Science, Bangalore
Mayya Y.D., 1995, AJ 109, 2503
Myers P.C., Dame T.M., Thaddeus P., et al., 1986, ApJ 301, 398
Osterbrock D.E., 1989, Astrophysics of Gaseous Nebulae and Active Galactic Nuclei. University Science Books, California
Phillips M.M., Jenkins C.R., Dopita M.A., Sadler E.M., Binette L., 1986, AJ 91, 1062
Prabhu T.P., Mayya Y.D., Anupama G.C., 1992, J. Astron. Astrophys. 13, 129
Roberts M.S., Hogg D.E., Bregman J.N., Forman W.R., Jones C., 1991, ApJS 75, 751
Shields J.C., 1991, AJ 102, 1314
Shuder J.M., 1981, ApJ 244,12
Singh K.P., Prabhu T.P., Kembhavi A.K., Bhat P.N., 1994, ApJ 424, 638
Sparks W.B., Macchetto F., Golombek D., 1989, ApJ 345, 153
Stanger V.J., Warwick R.S., 1986, MNRAS 220, 363
Stetson P.B., 1987, PASP 99, 191
Stone R.P.S., 1977, ApJ 218, 767
Thomas P.A., Fabian A.C., Arnaud K.A., Forman W., Jones C., 1986, MNRAS 222, 655
Trinchieri G., di Serego Alighieri S., 1991, AJ 101, 1647 (TdSA)
Vennik J., 1986, Astron. Nachr. 307, 157
Wampler E.J., 1992, ESO Messenger, West R.M. (ed.), 70, 82